Cubic polynomial curve-guided method for isochromatic determination in three-fringe photoelasticity

Xiaomeng Liu (刘晓蒙)* and Shuguang Dai (戴曙光)

School of Optical Electrical and Computer Engineering, University of Shanghai for Science and Technology, Shanghai 200093, China

**Corresponding author: lxm798@163.com*

Received June 6, 2015; accepted August 19, 2015; posted online September 17, 2015

A method for isochromatic determination in three-fringe photoelasticity is presented. It combines the phase-shifting method with cubic polynomial curve-fitting technology to eliminate the errors caused by color repetition. We perform a demonstration of the method on a circular disc subjected to compressive loading and an injection-molded cover with residual stresses. The test results compare well with the theoretical results.

OCIS codes: 120.0120, 120.5050.
doi: 10.3788/COL201513.101202.

Photoelasticity is one of the most widely used experimental methods for whole-field stress analysis in mechanics[1]. The isochromatic and isoclinic fringes correspond to the principal stress differences and their orientations, respectively. Many techniques have been developed to evaluate isochromatic fringes; they can be broadly classified into phase shifting, spectral content analysis, and the Fourier transform approach[2]. Among the various techniques, red, green, and blue (RGB) photoelasticity[3] is a useful photoelastic technique to obtain full-field isochromatic data. Since color merging occurs in RGB photoelasticity beyond three fringe orders when generic white light sources are used, it is also known as three-fringe photoelasticity (TFP)[4,5].

The isochromatic fringe order at an interesting point in the actual model is established by comparing the values of R, G, and B at the point of interest with the calibration table. Ideally, the same test specimen and lighting conditions are used in both the calibration and the application experiments, but this is not possible in some applications. Color adaptation[6,7] is a simple way of suitably modifying the calibration table. TFP was originally used to estimate total fringe orders up to a value of three, as beyond this point, the colors tend to merge; however, there have been attempts to push this limit[8,9].

Although the basic principle of TFP is not complicated, it is difficult to accurately estimate all of the parameters in practice, such as quarter-wave plate error, dispersion of the stress-optic coefficient, the spectral response of the camera, the spectral composition of the light source, and the transmission response of the polariscope components[10]. The evaluation of fringe orders using the least square error method is quite simple; however, it is prone to error at some locations owing to the repetition of colors[11]. This is a major problem in TFP.

This Letter concentrates on the determination of isochromatic fringe orders using a plane polariscope with a white light source. In this case, the isochromatic fringe is not affected by the isoclinic fringe or the quarter-wave plate error, which occurs when using a circular polariscope[12]. Moreover, the influence of background light is eliminated. A new scanning scheme is proposed to determine the isochromatic fringe orders. The applicability of the new method in determining the fringe orders of a loaded disc and an injection-molded cover with residual stresses is demonstrated.

In conventional TFP, researchers use a circular polariscope with a white light source to obtain the full-field isochromatic data[13]. As Fig. 1(a) shows, in white light, the intensity emerging from a dark-field circular polariscope ($\alpha = 90°$, $\xi = 135°$, $\phi = 45°$, and $\beta = 0°$) can be written as[5]

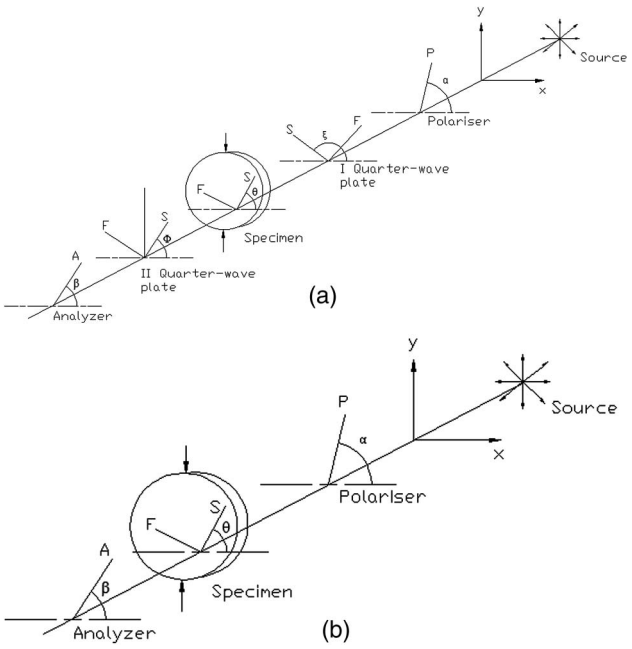

Fig. 1. Optical arrangements: (a) circular polariscope and (b) plane polariscope.

$$I_d = I_b + \frac{1}{\lambda_2 - \lambda_1}\int_{\lambda_1}^{\lambda_2} F(\lambda)\,T(\lambda)I_0(\lambda) \times \sin^2\frac{\delta(\lambda)}{2}(1-\cos^2 2\theta\sin^2\varepsilon)\mathrm{d}\lambda\ , \quad (1)$$

where I_b is the intensity of the background light, and $I_0(\lambda)$ accounts for the amplitude of the light vector. $F(\lambda)$ and $T(\lambda)$ represent the spectral responses of the camera and optical elements, respectively. λ_1 and λ_2 are the spectral limits of the light source or the camera, whichever is lower. $\delta(\lambda)$ is the retardation and θ is the isoclinic angle of the specimen. When white light is used, the quarter-wave plate no longer provides a phase shift of $\pi/2$ for all wavelengths, and in general behaves like a retarder. ε represents the error introduced by the quarter-wave plate. λ is the wavelength of the light.

Equation (1) shows the effect of the quarter-wave plate error, which depends upon the isoclinic angle θ. In order to minimize the influence of the quarter-wave plate error, Ajovalasit *et al.*[12] suggested that the calibration be performed with $\theta = 22.5°$. However, if the calibration table and the point of interest have different isoclinic angles θ, the obtained isochromatic data is not accurate.

The intensity of the light transmitted through a plane polariscope in a dark-field arrangement with white light as an illumination source[5] is given by

$$I_p = I_b + \left[\frac{1}{\lambda_2-\lambda_1}\int_{\lambda_1}^{\lambda_2} F(\lambda)\,T(\lambda)I_0(\lambda) \times \sin^2\frac{\delta(\lambda)}{2}\mathrm{d}\lambda\right]\sin^2 2(\theta-\beta_r), \quad (2)$$

where β_r is the angle between the analyzer and the x axis. By letting I_w represent the intensity of the isochromatic fringe field, we obtain

$$I_w = \frac{1}{\lambda_2-\lambda_1}\int_{\lambda_1}^{\lambda_2} F(\lambda)\,T(\lambda)I_0(\lambda)\sin^2\frac{\delta(\lambda)}{2}\mathrm{d}\lambda. \quad (3)$$

Equation (2) can be written as

$$I_p = I_b + I_w\sin^2 2(\theta-\beta_r). \quad (4)$$

The phase-shifting technique can be applied in TFP[14,15]. Petrucci[16] used a four-step approach for isochromatic determination in a plane polariscope with white light; with this method, a set of four images with $\beta_r = r\times 22.5°\ (r = 0,1,2,3)$ are obtained. The isochromatic intensity field can be separated from the isoclinic using

$$I_{wj} = \sqrt{(I_{2,j}-I_{0,j})^2 + (I_{3,j}-I_{1,j})^2} \qquad (j = R, G, B). \quad (5)$$

where $I_{r,j}(r = 0,1,2,3; j = R, G, B)$ correspond to pixel gray levels of the *R*-, *G*-, and *B*- planes for the analyzer positions of 0, 22.5°, 45°, and 67.5°, respectively. I_{wR}, I_{wG}, and I_{wB} are the R, G, and B values to be used in TFP to find the total fringe order.

Due to the facts that the isoclinic parameter does not depend on the wavelength and a plane polariscope is use for imaging, the isochromatic is not affected by the quarter-wave plate error, and the background light is eliminated too. These advantages would greatly enhance the application of TFP in an industrial scenario.

During the analysis, the values of R_e, G_e, and B_e at pixels in the specimen where the retardation has to be determined and the values of R_i, G_i, and B_i stored in the calibration table are calculated using Eq. (5). The retardation corresponding to each set of R_e, G_e, and B_e values can be evaluated by a comparison with the calibration table. The general procedure consists of the following:

1. Comparing the R_e, G_e, and B_e values of the specimen with the R_i, G_i, and B_i values stored in the calibration table by means of the error function, which is defined as

$$e_i = (R_i - R_e)^2 + (G_i - G_e)^2 + (B_i - B_e)^2, \quad (6)$$

for each index i of the calibration table[3]. $i = 1, ..., i_m$, i_m is the number of the RGB values in the calibration table.

2. Searching the value of the index i for which e_i is the minimum; therefore, the fringe order corresponding to i would be the resolved fringe order.

Due to the wide wavelength spectrum response of the CCD, the repetition of colors is observed in different ranges of fringe orders[11]. It leads to the false evaluation of the fringe orders. The variation of principal stress is continuous and this has to be judiciously used to order fringes; therefore, the problem can be solved by imposing fringe order continuity. Many investigators have proposed various methodologies[17]. Ramesh[11] introduced the refined TFP (RTFP) method, where the performance of the algorithm is controlled by parameter K, in which Eq. (6) is modified as

$$e_i = \sqrt{(R_i-R_e)^2+(G_i-G_e)^2+(B_i-B_e)^2+(N_p-N)^2\times K^2}, \quad (7)$$

where the additional term N_p is the fringe order obtained for the neighborhood pixel to the point under consideration in the specimen, and N is the fringe order at the current checking point of the calibration table. Ajovalasit *et al.*[8] proposed a window search method for isochromatic fringe orders determination. The advantage of this method is that the user need not select any parameter to control the performance of the algorithm. In the window search method, only a small window centered on the previously resolved pixel is searched in the calibration table. The window search method can be expressed as

$$e_i = \sqrt{(R_i - R_e)^2 + (G_i - G_e)^2 + (B_i - B_e)^2};$$
$$i \in [i_c - \Delta i, i_c + \Delta i], \tag{8}$$

where i_c is the calibration table index corresponding to the correct value of the retardation in the neighborhood of the pixel to be resolved, and Δi is the search window size. The window search method can assure the spatial continuity of the fringe order.

In the RTFP method, the user should find a neighbor whose fringe order is correct and assume this point as N_p in Eq. (7) to start the fringe demodulation. In the window search method, the start pixel should be the correctly resolved pixel in the neighborhood of the pixel to be resolved. Therefore, these techniques have the limitation of a priori knowledge of the start point to determine the fringe orders. In this Letter, a simpler technique of isochromatic determination that is based on the cubic polynomial curve-guided method is presented.

Using the four-step approach in a plane polariscope with white light as a source, the calibration table containing the RGB values associated with known fringe orders can be prepared using a beam under four-point bending[5]. The influence of the fringe gradient could be incorporated easily by appropriately selecting the bending load. To demonstrate the new method, three calibration tables corresponding to 0–1, 0–2, and 0–3 fringe orders are to be obtained. In order to make the system more robust, the procedure is repeated for 100 transverse lines, and the averaged results are saved in the calibration table. Three calibration tables are to be searched until the error e_i is at a minimum.

The experiment was performed on a disk under diametrical compression. The calibration beam and experimental disk are made of polycarbonate, with a material fringe value of $F_\sigma = 7.8$ N/mm/fringe. The disk is 35 mm in diameter and 4 mm thick under a load P of 196 N. An RGB camera with a resolution of 2452×2056 pixels is used. Four images using the four-step approach are digitized as shown in Fig. 2, and the whole-field isochromatic is obtained using Eq. (5). Figure 3(a) shows the resolved isochromatic fringe orders using Eq. (6) with masked regions, as the maximum resolvable fringe order in this Letter is three. Figure 3(b) shows the fringe order variation along the line cd in Fig. 3(a). Due to the repetition of colors, point R in Fig. 3(b) has an incorrect fringe order. The variation of the error e_i of point R using Eq. (6) is shown in Fig. 3(c). One can observe that the value e_A at point A is the least, but the correct fringe order is seen at point B. In order to obtain the correct isochromatic fringe orders, the preceding mentioned search procedure should be modified.

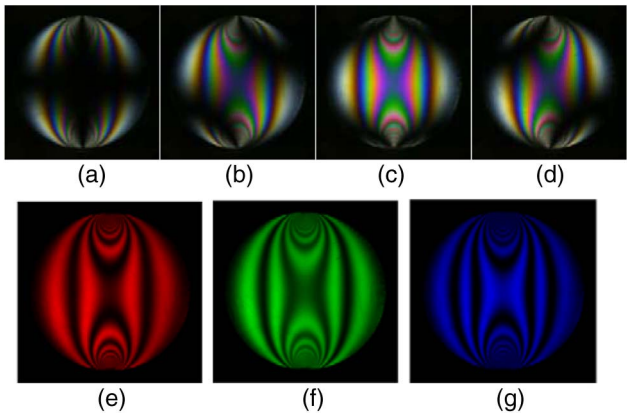

Fig. 2. Experimentally obtained images of a disc under diametrical compression using the four-step approach: (a)–(d) I0–I3. (e)–(g). Fringe maps of R, G, and B planes calculated using Eq. (5).

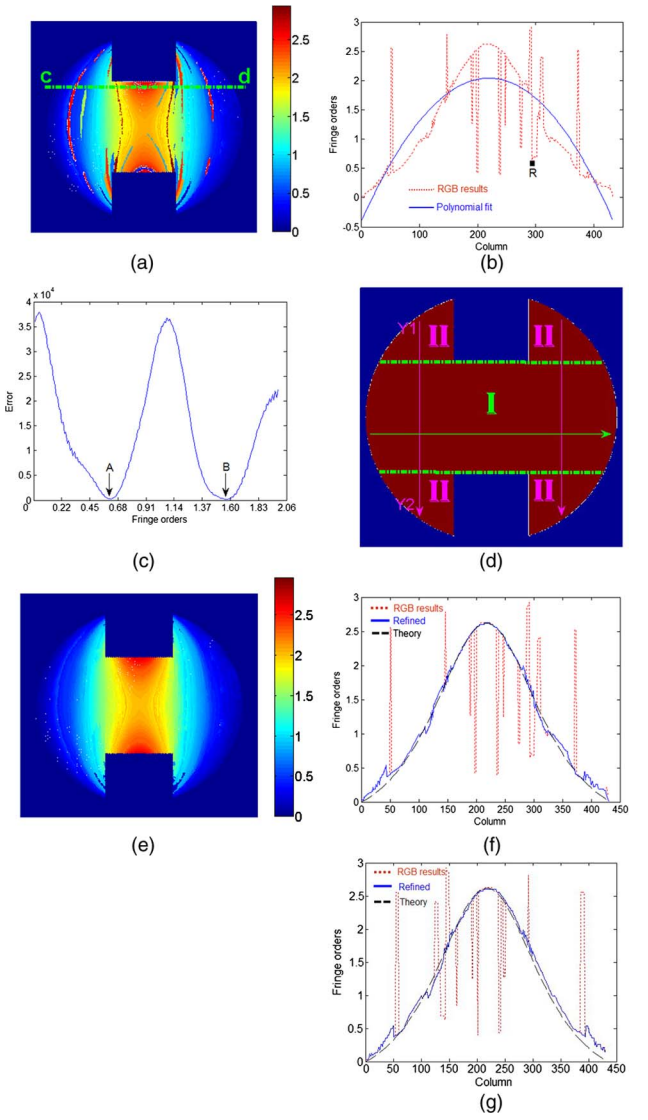

Fig. 3. (a) Resolved isochromatic fringe orders using Eq. (6). (b) Fringe order variation along line cd and the fitted curve. (c) Variation of e_i of point R using Eq. (6). (d) Separated parts for isochromatic determination. (e) Whole-field refined results. (f) RGB results, refined results, and theoretical results along line cd; (g) RGB results, refined results, and theoretical results along line cd using a circular polariscope arrangement following Ajovalsit *et al.*

Grewal *et al.*[18] used piecewise continuity and polynomial curve-fitting methods for isochromatic data smoothing. Although polynomial curve fitting is a good algorithm for noise separation, the original values of the isochromatic fringe orders even at the point of correct demodulation have been changed by the data smoothing method.

A cubic polynomial was fitted to the data of the calculated fringe orders of line cd, as shown in Fig. 3(b). The difference between the fringe orders and fitted curve is calculated, and if we set a threshold value to the difference, the incorrect point R can be easily identified. For point R, the error array e_i is to be searched again, excluding point A until the error is at a minimum. The implementation procedure of the cubic polynomial curve-guided method for isochromatic determination is shown in the flowchart in Fig. 4. Initially, the fringe orders are obtained using Eqs. (5) and (6) over the model domain, and then a threshold value has to be set. The value of 0.5 is found to be suitable for most purposes. Refinement is performed only for the incorrect fringe order points. The advantage of this method is that the user need not select a seed point to start the refinement[11].

In this demonstration, because the disk is masked, the refinement in Fig. 3(a) is separated into two parts, which are shown in Fig. 3(d). Firstly, part I is evaluated in every horizontal line, and then part II is evaluated in every vertical line (taken along the entire line from Y1 to Y2). In every horizontal line and vertical line in Fig. 3(a), a cubic polynomial is fitted to the data to obtain an equation to determine the fringe orders. The threshold value is set to 0.5 in this Letter. Whole-field refined fringe orders mapped with the masked regions is shown in Fig. 3(e). As Fig. 3(e) shows, the refined results are achieved where the incorrect isochromatic fringe orders are eliminated, as compared to the evaluated fringe orders using Eq. (6). Figure 3(f) compares the evaluated fringe orders using Eq. (6) and the refined results obtained for the line cd in Fig. 3(a). One can see that only the abrupt jump section of the results is modified, clearly illustrating the efficacy of the technique to eliminate peak errors while preserving the originally demodulated correct fringe orders. The theoretical results are shown in Fig. 3(f), as well. The refined results obtained using the cubic polynomial curve-guided method along line cd agree well with the theoretical results.

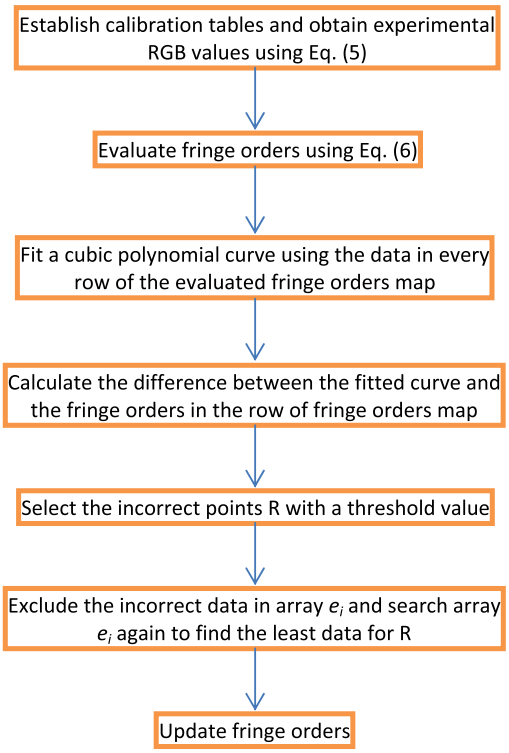

Fig. 4. Procedure of isochromatic determination.

Capturing four phase-shifted images is difficult in dynamic applications. Researchers used a circular polariscope in the dark field under white light to obtain isochromatic fringe patterns in one image. The errors caused by the repetition of colors in the circular polariscope arrangement also can be eliminated using the proposed method. For the same specimen and loading conditions in a plate polariscope, a circular polariscope is performed following the arrangement of Ajovalsit *et al.*[12]. The fringe orders from the circular polariscope analysis along the same line as reported in Fig. 3(a) are shown in Fig. 3(g).

The other problem of an injection-molded polycarbonate cover is used to explain the method. Injection-molded articles usually possess residual stresses[19,20]. The

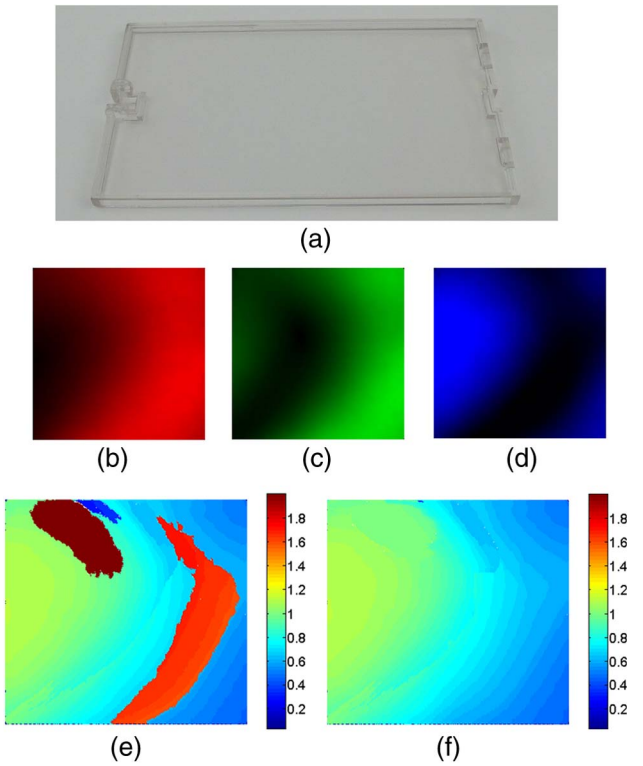

Fig. 5. (a) Injection-molded polycarbonate cover. (b)–(d) Fringe maps of R, G, and B planes in the center part of the cover calculated using Eq. (5). (e) Resolved fringe orders using Eq. (6). (f) Refined fringe orders.

rectangular cover with a flat surface at the center part is shown in Fig. 5(a) (length 90 mm, breadth 55 mm, thickness 2 mm). A square area the size of 30 mm × 30 mm in the center part of the cover is chosen to evaluate the fringe orders. Initially, the isochromatic fringe is obtained using Eq. (5) and the fringe orders are calculated using Eq. (6), as shown in Fig. 5(e). Then, the refined results achieved using the cubic polynomial guided method are shown in Fig. 5(f). As Fig. 5(f) shows, the refined results are achieved where the most incorrect isochromatic fringe orders are eliminated, proving that the performance of the method is good for isochromatic fringe orders determination.

The polynomial curve-guided method is effective for continuous isochromatic determination. For the problems involved in complex fringe patterns, a higher-order polynomial is recommended and the threshold value is selected iteratively according to the results of the refinement. The choice of scanning direction in a given problem depends on the zone of noise and its shape. Our experiments show that the scanning direction perpendicular to the noise streaks is effective in reducing errors.

In conclusion, a new method is proposed for isochromatic determination in TFP. The refinement scheme developed using this method assures stress continuity and does not change the original values of the isochromatic fringe at the point of correct demodulation. Furthermore, the technology does not need to select any seed points to start refinement.

This work was supported by the Innovation Fund Project for Graduate Students of Shanghai under Grant No. JWCXSL1301. We acknowledge the reviewers for their helpful comments and critiques.

References

1. Department of Material Mechanics Photoelastic Group of Tianjin University, *Principle of Photoelasticity and Test Technology* (in Chinese) (Science Press, 1980).
2. M. Ramji, E. Nithila, K. Devvrath, and K. Ramesh, Sādhanā **33**, 27 (2008).
3. A. Ajovalasit, S. Barone, and G. Petrucci, Exp. Mech. **35**, 193 (1995).
4. K. Ramesh and S. S. Deshmukh, Strain **32**, 79 (1996).
5. K. Ramesh, *Digital Photoelasticity Advanced Techniques and Applications* (Springer–Verlag, 2000).
6. B. N. Simon, T. Kasimayan, and K. Ramesh, Exp. Tech. **35**, 59 (2011).
7. D. Swain, B. P. Thomas, J. Philip, and S. A. Pillai, Exp. Mech. **55**, 1031 (2015).
8. A. Ajovalasit, G. Petrucci, and M. Scafidi, Strain **46**, 137 (2010).
9. D. Swain, B. P. Thomas, and J. Philip, Opt. Eng. **54**, 081204 (2015).
10. J. A. Quiroga, A. García-Botella, and J. A. Gómez-Pedrero, Appl. Opt. **41**, 3461 (2002).
11. K. R. Madhu and K. Ramesh, Opt. Lasers Eng. **45**, 175 (2007).
12. A. Ajovalasit, S. Barone, and G. Petrucci, J. Strain Anal. Eng. Des. **30**, 29 (1995).
13. S. Kale and K. Ramesh, Opt. Lasers Eng. **51**, 592 (2013).
14. K. Ramesh and S. S. Deshmukh, Opt. Lasers Eng. **28**, 47 (1997).
15. A. Ajovalasit, G. Petrucci, and M. Scafidi, Opt. Lasers Eng. **45**, 596 (2007).
16. G. Petrucci, Exp. Mech. **37**, 420 (1997).
17. K. Ramesh, T. Kasimayan, and B. Neethi Simon, J. Strain Anal. Eng. Des. **46**, 245 (2011).
18. G. S. Grewal, V. N. Dubey, and D. J. Claremont, Strain **42**, 273 (2006).
19. Z. Zhang, H. Liu, J. Huang, X. Zhou, X. Cheng, X. Jiang, W. Wu, and W. Zheng, Chin. Opt. Lett. **11**, 041402 (2013).
20. S. Deng, F. Wang, S. Liu, G. Li, L. Sun, and Y. Jin, Chin. Opt. Lett. **11**, S10701 (2013).